

# Determination of beta-delayed neutron emission probability limits of rhodium isotopes by gamma-ray spectroscopy

R Shearman<sup>1,2</sup>, G Lorusso<sup>1,2,3</sup>, A Boso<sup>1</sup>, P H Regan<sup>1,2</sup>,  
 S Nishimura<sup>3,4</sup>, Z Y Xu<sup>3,5,6</sup>, A Jungclaus<sup>7</sup>, Y Shimizu<sup>3</sup>, G S Simpson<sup>8</sup>,  
 P-A Söderström<sup>3</sup>, H Watanabe<sup>3,9</sup>, F Browne<sup>3,10</sup>, P Doornenbal<sup>3</sup>,  
 G Gey<sup>3,8</sup>, H S Jung<sup>11</sup>, B Meyer<sup>12</sup>, T Sumikama<sup>13</sup>, J Taprogge<sup>3,7,14</sup>,  
 Zs Vajta<sup>3,15</sup>, J Wu<sup>3,16</sup>, H Baba<sup>3</sup>, G Benzoni<sup>17</sup>, K Y Chae<sup>18</sup>,  
 F C L Crespi<sup>17,19</sup>, N Fukuda<sup>3</sup>, R Gernhäuser<sup>20</sup>, N Inabe<sup>3</sup>, T Isobe<sup>3</sup>,  
 T Kajino<sup>4,21</sup>, D Kameda<sup>3</sup>, G D Kim<sup>22</sup>, Y-K Kim<sup>22,23</sup>, I Kajouharov<sup>24</sup>,  
 F G Kondev<sup>25</sup>, T Kubo<sup>3</sup>, N Kurz<sup>24</sup>, Y K Kwon<sup>22</sup>, G J Lane<sup>26</sup>, Z Li<sup>16</sup>,  
 A Montaner-Pizá<sup>27</sup>, K Moschner<sup>28</sup>, F Naqvi<sup>29</sup>, M Niikura<sup>5</sup>,  
 H Nishibata<sup>30</sup>, A Odahara<sup>30</sup>, R Orlandi<sup>31</sup>, Z Patel<sup>2</sup>, Zs Podolyák<sup>2</sup>,  
 H Sakurai<sup>3,5</sup>, H Schaffner<sup>24</sup>, P Schury<sup>3</sup>, S Shibagaki<sup>4,21</sup>, K Steiger<sup>20</sup>,  
 H Suzuki<sup>3</sup>, H Takeda<sup>3</sup>, A Wendt<sup>28</sup>, A Yagi<sup>30</sup>, K Yoshinaga<sup>32</sup>

<sup>1</sup>National Physical Laboratory, Teddington, Middlesex, TW11 0LW, UK

<sup>2</sup>Department of Physics, University of Surrey, Guildford, GU2 7XH, UK

<sup>3</sup>RIKEN Nishina Center, 2-1 Hirosawa, Wako-shi, Saitama 351-0198, Japan

<sup>4</sup>Division of Theoretical Astronomy, NAOJ, 181-8588 Mitaka, Japan

<sup>5</sup>Department of Physics, University of Tokyo, Hongo, Bunkyo-ku, Tokyo, 113-0033, Japan

<sup>6</sup>Department of Physics, University of Hong Kong, Pokfulam Road, Hong Kong

<sup>7</sup>Instituto de Estructura de la Materia, CSIC, E-28006 Madrid, Spain

<sup>8</sup>LPSC, Université Joseph Fourier Grenoble 1, CNRS/IN2P3, Institut National Polytechnique de Grenoble, F-38026 Grenoble Cedex, France

<sup>9</sup>IRCNPC, School of Physics and Nuclear Energy Engineering, Beihang University, Beijing 100191, China

<sup>10</sup>School of Computing, Engineering and Mathematics, University of Brighton, BN2 4GJ, UK

<sup>11</sup>Department of Physics, Chung-Ang University, Seoul 156-756, Republic of Korea

<sup>12</sup>Department of Physics and Astronomy, Clemson University, South Carolina 29634, USA

<sup>13</sup>Department of Physics, Tohoku University, Aoba, Sendai, Miyagi 980-8578, Japan

<sup>14</sup>Departamento de Física Teórica, Universidad Autónoma de Madrid, E-28049 Madrid, Spain

<sup>15</sup>Institute for Nuclear Research, Hungarian Academy of Sciences, P.O. Box 51, Debrecen H-4001, Hungary

<sup>16</sup>Department of Physics, Peking University, Beijing 100871, China

<sup>17</sup>INFN Sezione di Milano, I-20133 Milano, Italy

<sup>18</sup>Department of Physics, Sungkyunkwan University, Suwon 440-746, Republic of Korea

<sup>19</sup>Dipartimento di Fisica dell'Università degli Studi di Milano, I-20133 Milano, Italy

<sup>20</sup>Physik Department E12, Technische Universität München, D-85748 Garching, Germany

<sup>21</sup>Department of Astronomy, University of Tokyo, Hongo, Bunkyo-ku, Tokyo 113-0033, Japan

<sup>22</sup>Institute for Basic Science, Rare Isotope Science Project, Yuseong-daero

1689-gil, Yuseong-gu, 305-811 Daejeon, Republic of Korea

<sup>23</sup>Department of Nuclear Engineering, Hanyang University, Seoul 133-791, Republic of Korea

<sup>24</sup>GSI Helmholtzzentrum für Schwerionenforschung GmbH, 64291 Darmstadt, Germany

<sup>25</sup>Physics Division, Argonne National Laboratory, Argonne, Illinois 60439, USA



<sup>26</sup>Department of Nuclear Physics, R.S.P.E., Australian National University, Canberra, Australian Capital Territory 0200, Australia

<sup>27</sup>Instituto de Física Corpuscular, CSIC-University of Valencia, E-46980 Paterna, Spain

<sup>28</sup>Institut für Kernphysik, Universität zu Köln, Zùlpicher Strasse 77, D-50937 Köln, Germany

<sup>29</sup>Wright Nuclear Structure Laboratory, Yale University, Connecticut 06520-8120, USA

<sup>30</sup>Department of Physics, Osaka University, Machikaneyama-machi 1-1, Osaka 560-0043, Japan

<sup>31</sup>Instituut voor Kern en Stralingsfysica, KU Leuven, B-3001 Leuven, Belgium

<sup>32</sup>Department of Physics, Tokyo University of Science, 2641 Yamazaki, Chiba 278-8510, Japan

E-mail: robert.shearman@npl.co.uk

October 2019

**Abstract.** The decay of five neutron-heavy rhodium isotopes were studied at the Radioactive Isotope Beam Factory (RIBF) Facility at the RIKEN Nishina Center after relativistic fission of  $^{238}\text{U}$  beam on a thick beryllium target. Previously unknown associated gamma-ray decay energies are reported for each nuclide, and through evaluating the intensity of the  $2^+ \rightarrow 0^+$  E2 transition in the even-even palladium daughter nuclei,  $^{120,122,124}\text{Pd}$ , from the beta-tagged gamma-ray spectra an upper or lower limit of beta-delayed neutron emission is deduced for each nuclei. A general, expected trend of increasing  $P_n$  is observed in the direction of the neutron drip line.

## 1. Introduction

Trends in bulk decay parameters across isotopic chains can reveal deeper insight into the evolving dynamics of nuclear matter. Rhodium, the 45<sup>th</sup> element in the periodic table, is five holes short of the proton shell closure, and with large exoticism can cross the N=82 shell closure. In this respect the bulk decay parameters of rhodium are of enhanced interest. The probability of the beta-delayed neutron emission is one such bulk characteristic which can elucidate the understanding of regions within the Segré chart. Emissions of this type not only relate to the neutron separation energy of the daughter nuclei and the  $Q_\beta$  value of the decay but also to the shell structure of the daughter and the possible channels open near the Fermi surface for beta coupling.

## 2. Experimental setup

The decay studies of rhodium isotopes have been performed at the RIBF facility at the RIKEN Nishina Center. Neutron rich nuclei were produced by the fast fission of an accelerated (345 MeV/u)  $^{238}\text{U}^{86+}$  ion impinged on a beryllium target of 3 mm thickness. The uranium was accelerated using a 5 stage LINAC-Cyclotron accelerator, detailed in [1].

Fragments were identified and separated using the BigRIPS and ZeroDegree spectrometers, which using in-line detectors derived the A/Q and the charge of the fragment with ample precision for different nuclei to be well resolved. Plotting the mass to charge against the charge of the fragments allows for the creation of a Particle IDentification plot, from which gates can be set to select specific species, see figure 1.

Ions are implanted onto the double-sided stacked silicon detector (DSSSD), WAS3ABi [2]. Gamma rays were detected using EURICA [3], closely packed around the beta and ion detector. From this detector suite ion-beta-gamma correlations can be created and gamma rays associated to particular nuclide decay can be identified. Deriving the limit of the  $P_n$  value, the branching of the decay to beta-delayed neutron emission, is calculated as the ratio of decays of the parent nuclei to the population of the even-even daughter, depending on the oddness of the parent this ratio is either the  $P_n$  or  $1 - P_n$ . The beta delayed neutron branching limit is calculated on the assumption that in the even-even daughter nucleus, the yrast  $2^+ \rightarrow 0^+$  transition is fed every

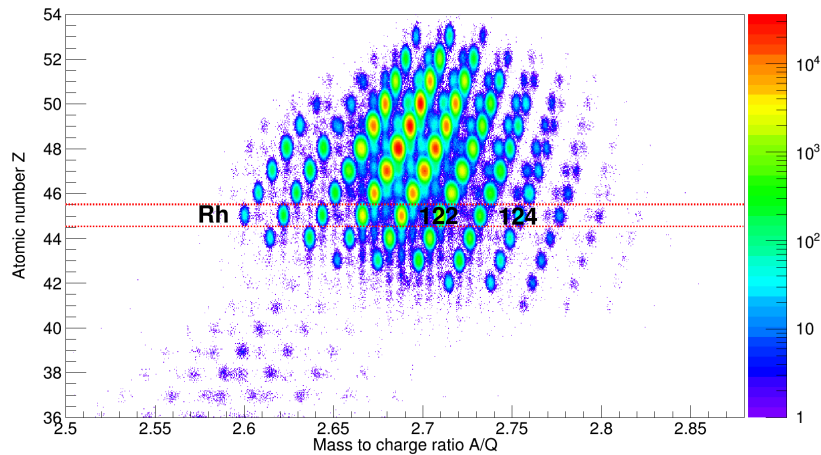


Figure 1: Particle identification plot of the species populated during the RIBF experimental campaign, specific ions are well resolved.

decay. Asserting that this transition is not attenuated significantly by the construction of WAS3ABi itself and from knowing the efficiency of EURICA in this geometry the strength of this transition can be derived. The number of implanted ions of a particular nuclei, is calculated from the beta-ion time spectrum. Fitting this spectrum with the Bateman equations allows for the number of decays of the parent nuclei, the implanted ion, to be calculated.

### 3. Results

#### 3.1. $^{120}\text{Rh}$

There has only been one previous study of the decay of  $^{120}\text{Rh}$  performed at the NSCL at MSU, [4]. All de-populations observed are confirmed in this work. The 438 keV gamma ray, assigned as the  $2^+ \rightarrow 0^+$  yrast transition is observed as the strongest fed transition. The number of decays extracted from the final fit of the implanted spectrum numbered  $10^5$ , and the parent half-life calculated to be 140(5) ms, which is in agreement with [5]. The time gate of the accompanying gamma-ray spectrum was set to 480 ms, at this value 90 % of the parent nuclide has decayed but only a third of the daughter nuclei, enhancing the signal to noise, whilst preserving the statistics in the peaks of interest.

The  $\beta$  correlated gamma-ray spectrum of decay of  $^{120}\text{Rh}$  is shown in figure 2, also shown is a normalised correlated spectrum from the decay of the  $^{120}\text{Pd}$ , and a spectra created through the subtraction of the daughter dataset. The remaining lines, are de-excitations from  $^{120}\text{Pd}$  itself or are from the  $\beta - n$  channel. The originations of the gamma rays were confirmed by  $\gamma - \gamma$  coincidences also shown in 2. The peak areas of the seven gamma rays assigned to the direct  $\beta$  decay of  $^{120}\text{Rh}$  were calculated, intensities relative to the  $2^+ \rightarrow 0^+$  transition determined, and absolute gamma-ray intensities calculated. Finally the absolute decay intensity for the  $2^+ \rightarrow 0^+$  transition, corrected for internal conversion, was used to give an upper limit on the  $\beta - n$  decay probability to  $^{119}\text{Pd}$ , from the missing intensity in the transition. These results are presented in table 1.

The gamma ray transitions seen in coincidence with the 436 keV transition agree with the previously reported gamma rays by Stoyer et al., [6], with slight disagreements in gamma-ray energy (2 keV for the 436 keV transition). This work did not see the 881 keV or 824 keV transitions believed to depopulate the yrast  $10^+$  in  $^{120}\text{Pd}$ , however three gamma rays previously unreported have been observed for the first time. The 129 keV, 465 keV and 900 keV transition,

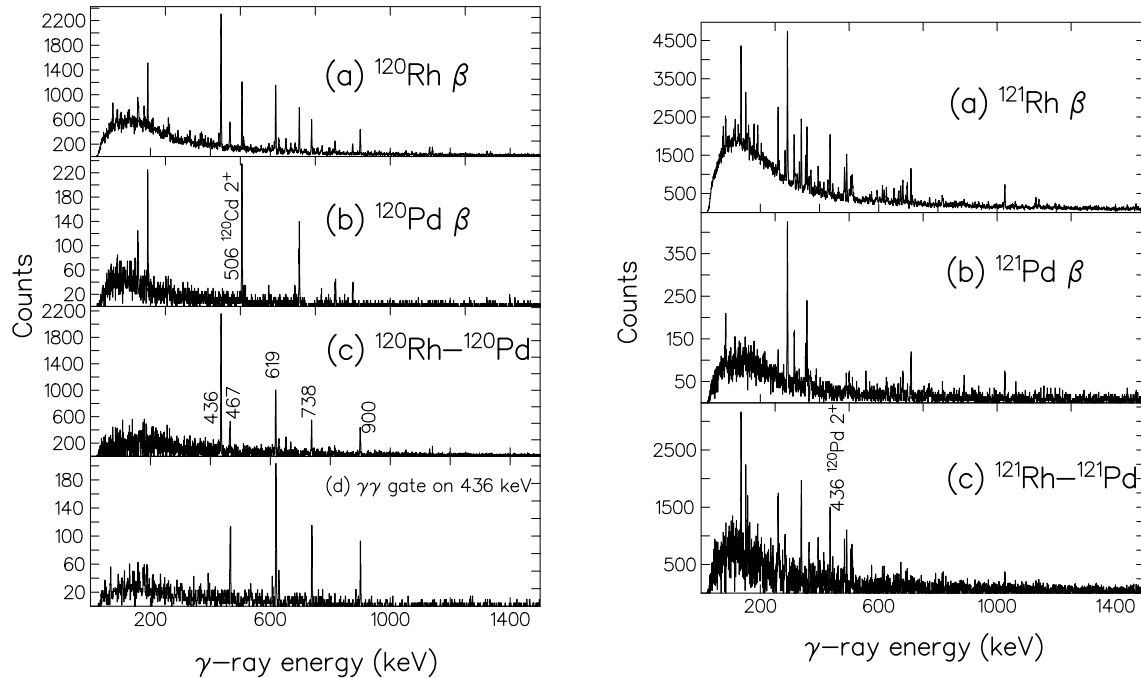


Figure 2: LEFT: Gamma-ray spectra associated with the decay of (a)  $^{120}\text{Rh}$  and (b)  $^{120}\text{Pd}$ . (c) A  $^{120}\text{Pd}$  subtracted  $^{120}\text{Rh}$  spectrum showing events associated with the primary decay of  $^{120}\text{Rh}$  only, which are assumed to be gamma-ray transitions from excited states in the  $^{120}\text{Pd}$  daughter nucleus. (d) Gamma-ray coincidence spectra gated on the 436 keV  $2^+ \rightarrow 0^+$  transition in  $^{120}\text{Pd}$ . The  $\beta - \gamma$  correlation times for each of these spectra was 2.350 s.

RIGHT: Gamma-ray spectra associated with the decay of (a)  $^{121}\text{Rh}$  and (b)  $^{121}\text{Pd}$ . (c) A  $^{121}\text{Pd}$  subtracted  $^{121}\text{Rh}$  spectrum showing events associated with the primary decay of  $^{121}\text{Rh}$ , which are assumed to be gamma-ray transitions from excited states in the  $^{120,121}\text{Pd}$  daughter nuclei. The  $\beta - \gamma$  correlation times for each of these spectra was 1.36 s.

$E_\gamma$ (keV)	$I^\pi \rightarrow I^\pi$	Relative $P_\gamma$	Absolute $P_\gamma$	Transition intensity	$P_n$
435.6	$2^+ \rightarrow 0^+$	1.00(4)	0.91(4)	0.91 (4)	$\leq 0.089$ (4)
617.9	$4^+ \rightarrow 2^+$	0.60(4)	0.541(23)	0.543 (23)	
737.6	$6^+ \rightarrow 4^+$	0.308(22)	0.278(16)	0.308 (22)	
795.9	-	0.0532(14)	0.048(13)		
899.8	-	0.303(25)	0.274(19)		
465.2	-	0.283(21)	0.256(15)		
129.3	-	0.06(4)	0.05(3)		

Table 1: Relative and absolute intensities of the gamma-rays identified to be associated with the excited levels of  $^{120}\text{Pd}$ . Tentative spin and parity assignments have been made for the two lowest lying states in agreement with [4]. The upper limit of the  $P_n$  value of this nuclide is calculated from the missing total intensity associated with the 435.6 keV emission.

which were all seen in coincidence with the 436 keV transition. The upper limit of the  $P_n$  for the decay of  $^{120}\text{Rh}$  was deduced to be 0.089(4) (i.e. 8.9 %); this upper limit is larger than reported than that by Montes et al., [7].

### 3.2. $^{121}\text{Rh}$

For the decay of  $^{121}\text{Rh}$ , the inverse is true for the determination of the  $P_n$ . In this case, the area of the  $2^+$  peak in the decay of  $^{120}\text{Pd}$  corresponds to the lower limit of the  $P_n$  value. The number of implanted  $^{121}\text{Rh}$  ions was on WAS3ABi was  $1.04(1)\times 10^5$ . The same 436 keV transition is used in the determination of the  $P_n$ , which in this case is populated via the  $\beta - n$  channel and thus is a lower limit of the branching equal to 0.115(6). Subtracting the daughter spectra allows for identification of gamma rays originating from the excited levels of  $^{121}\text{Pd}$  and  $^{120}\text{Pd}$ . These are summarized in table 2.

$E_\gamma$ (keV)	$I^\pi \rightarrow I^\pi$	Absolute $P_\gamma$	Transition intensity	$P_n$
135	-	0.154(5)		
150.5	-	0.074(4)		
283.5	-	0.051(4)		
338	-	0.146(4)		
396	-	0.052(3)		
483	-	0.065(4)		
493	-	0.098(4)		
681.4	-	0.022(3)		
435.6	$2^+ \rightarrow 0^+$	0.114(6)	0.115(6)	$\geq 0.115(6)$

Table 2: Absolute  $\gamma$ -ray emission probabilities,  $P_\gamma$ , values for the decay of  $^{121}\text{Rh}$ . From the transition intensity of the  $2^+ \rightarrow 0^+$  transition in  $^{120}\text{Rh}$ , a  $P_n$  lower limit of 0.115(6) has been determined for the decay of  $^{121}\text{Rh}$ .

The previously observed isomeric internal transition in  $^{121}\text{Rh}$  of 136 keV ( $T_1/2 = 46(9)$ ) [8] is observed strongly in this work. Seven further transitions observed in the decay of  $^{121}\text{Pd}$  are reported, but without placement in a level scheme. The value of the half-life calculated in this work, 71(7) ms agrees with [5].

### 3.3. $^{122}\text{Rh}$

Two excited levels of  $^{122}\text{Pd}$  have been previously observed by Wang et al., [9]. In that experiment at RIBF-Riken, a  $^{238}\text{U}$  beam was impinged upon 0.5 mm thick natural Tungsten target. Gamma rays from the de-excitations of the secondary beam were Doppler-corrected and measured using the DALI2 spectrometer [10]. 499(9) keV and 665(18) keV gamma rays were observed on the  $^{122}\text{Pd}$  gated spectrum and were identified as the first  $2^+ \rightarrow 0^+$  and  $4^+ \rightarrow 2^+$  transitions respectively. In the current work strongly-fed 513 keV and 674 keV gamma rays were observed, which were consistent with the results published from [9]. These transitions can be seen in figure 3, these gamma-ray spectra were created using a beta-ion correlation time window of 0.930 s. The proposed 513 keV  $2^+ \rightarrow 0^+$  transition was gated upon in  $\gamma\gamma$  coincidences, this spectrum is shown in (c) of figure 3. The deduced ion implants of  $1.12(5)\times 10^5$  for  $^{122}\text{Rh}$  allows for the absolute intensities of the detected gamma rays given in table 3, and for the upper limit of the  $\beta - n$  branching of the decay of  $^{122}\text{Rh}$  to be 0.0387(6).

### 3.4. $^{123}\text{Rh}$

Prior to the current work, no previous gamma rays have been reported for the decay of  $^{123}\text{Rh}$  to the excited states in  $^{123}\text{Pd}$ . The fitted time difference spectrum of the beta implantations

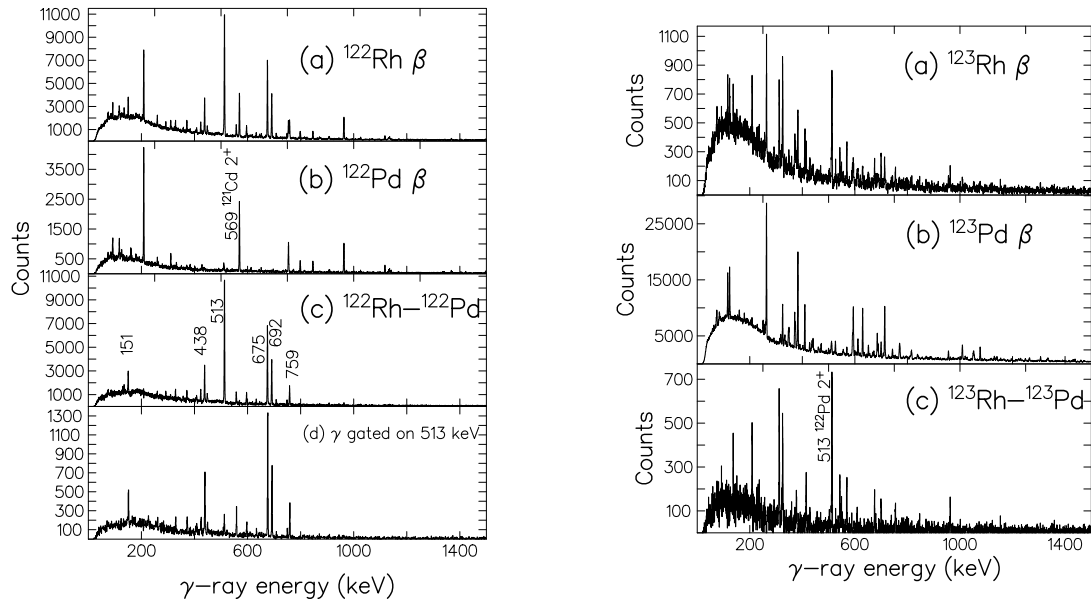


Figure 3: LEFT: Gamma-ray spectra associated with the decay of (a)  $^{122}\text{Rh}$  and (b)  $^{122}\text{Pd}$ . (c) A  $^{122}\text{Pd}$  subtracted  $^{122}\text{Rh}$  spectrum showing events associated with the primary decay of  $^{122}\text{Rh}$  only, which are assumed to be gamma-ray transitions from excited states in the  $^{122}\text{Pd}$  daughter nucleus. (d) Gamma-ray coincidence spectra gated on the 513 keV  $2^+ \rightarrow 0^+$  transition in  $^{122}\text{Pd}$ . The  $\beta - \gamma$  correlation times for each of these spectra was 0.930 s.

RIGHT: Gamma-ray spectra associated with the decay of (a)  $^{123}\text{Rh}$  and (b)  $^{123}\text{Pd}$ . (c) A  $^{123}\text{Pd}$  subtracted  $^{123}\text{Rh}$  spectrum showing events associated with the primary decay of  $^{123}\text{Rh}$  only, which are assumed to be gamma-ray transitions from excited states in the  $^{122,123}\text{Pd}$  daughter nuclei. The  $\beta - \gamma$  correlation times for each of these spectra was 0.910 s

$E_\gamma$ (keV)	$I^\pi \rightarrow I^\pi$	Relative $P_\gamma$	Absolute $P_\gamma$	Transition intensity	$P_n$
512.9	$2^+ \rightarrow 0^+$	1.00(16)	0.966(15)	0.961(15)	$\leq 0.0387(6)$
674.9	$4^+ \rightarrow 2^+$	0.686(16)	0.655(10)	0.657(10)	
691.0	-	0.0779(23)	0.0745(18)		
438.1	-	0.246(12)	0.236(11)		
150.1	-	0.112(9)	0.107(8)		
557.5	-	0.096(5)	0.092(5)		
758.3	-	0.17(3)	0.159(24)		
748.7	-	0.038(8)	0.036(8)		
448.3	-	0.072(8)	0.069(7)		

Table 3: Relative and absolute intensities of the gamma-rays identified to be associated with the excited levels of  $^{122}\text{Pd}$ . Tentative spin and parity assignments have been made for the two lowest lying states in agreement with [4]. The upper limit of the  $P_n$  value of this nuclide is also included calculated from the missing total intensity of the 513 keV emission.

determined that during the experiment  $2.73(3) \times 10^4$   $^{123}\text{Rh}$  ions were implanted. The subtracted spectra allows for identification of gamma rays associated with the excited levels of  $^{123}\text{Pd}$ , as

well as the  $2^+ \rightarrow 0^+$  in  $^{122}\text{Pd}$  to identified, from which the lower limit of the  $P_n$  is calculated as 0.255(14). Absolute intensities were determined for the de-excitation gamma rays observed in figure 3, these data are presented in table 4.

$E_\gamma$ (keV)	$I^\pi \rightarrow I^\pi$	Absolute $P_\gamma$	Transition intensity	$P_n$
136.8	-	0.05(7)		
414.4	-	0.064(9)		
543.1	-	0.051(4)		
548.6	-	0.30(6)		
512.9	$2^+ \rightarrow 0^+$	0.253(14)	0.255(14)	$\geq 0.255(14)$
674.9	$4^+ \rightarrow 2^+$	0.106(9)	0.106(9)	

Table 4: Absolute  $P_\gamma$  values for gamma ray emissions following the decay of  $^{123}\text{Rh}$ .

### 3.5. $^{124}\text{Rh}$

The most populated, intense gamma rays observed in the decay of  $^{124}\text{Rh}$  is the 588 keV and 702 keV lines, which can be tentatively assigned to the de-excitation of the  $2^+ \rightarrow 0^+$  and  $4^+ \rightarrow 2^+$  respectively. These assignments agree with the 590(11) keV and 710(19) keV decays noted in [9].

The assigned  $2^+ \rightarrow 0^+$  decay, coupled to the deduced ion implantation on WASABi of  $3.01(4) \times 10^3$ , were used to find an upper limit of the  $P_n$  value of 0.28(3). The nuclei was poorly populated in this campaign, however it was still possible to create  $\gamma\gamma$  coincidences from which the the origination of several weakly fed gamma rays could be resolved. This data is summarised in table 5.

$E_\gamma$ (keV)	$I^\pi \rightarrow I^\pi$	Relative $P_\gamma$	Absolute $P_\gamma$	Transition intensity	$P_n$
588.0	$2^+ \rightarrow 0^+$	1.00(9)	0.72(7)	0.72 (7)	$\leq 0.28$ (3)
701.8	$4^+ \rightarrow 2^+$	0.62(7)	0.44(5) (7)	0.44 (5)	
627.0	-	0.48(9)	0.34(6)		
232.8	-	0.22(5)	0.16(3)		

Table 5: Relative and absolute intensities of the gamma-rays identified to be associated with the excited levels of  $^{124}\text{Pd}$ . Tentative spin and parity assignments have been made for the two lowest lying states. The upper limit of the  $P_n$  value of this nuclide is also included calculated from the missing total intensity of the 588 keV emission.

## 4. Discussion

The deduced limits of the  $P_n$  values of five rhodium nuclei have been calculated, shown in 5. Four of these nuclei did not have limits or experimental values for the  $P_n$  before, the fifth limit for  $^{120}\text{Rh}$  is in agreement with the previous value, of  $\leq 5.4$  by Montes et al., [7]. An increasing  $P_n$  moving towards the neutron drip line is observed in these data. Further work is required, by using the granddaughter gamma-ray decays it is possible to deduce the  $P_n$  value and not the limit.

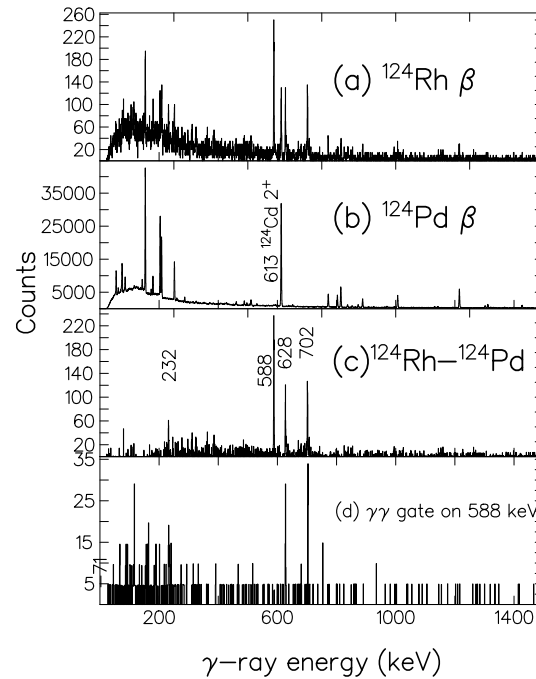


Figure 4: Gamma-ray spectra associated with the decay of (a)  $^{124}\text{Rh}$  and (b)  $^{124}\text{Pd}$ . (c) A  $^{124}\text{Pd}$  subtracted  $^{124}\text{Rh}$  spectrum showing events associated with the primary decay of  $^{124}\text{Rh}$  only, which are assumed to be gamma-ray transitions from excited states in the  $^{124}\text{Pd}$  daughter nucleus. (d) Gamma-ray coincidence spectra gated on the 588 keV  $2^+ \rightarrow 0^+$  transition in  $^{124}\text{Pd}$ . The  $\beta - \gamma$  correlation times for each of these spectra was 0.434 s.

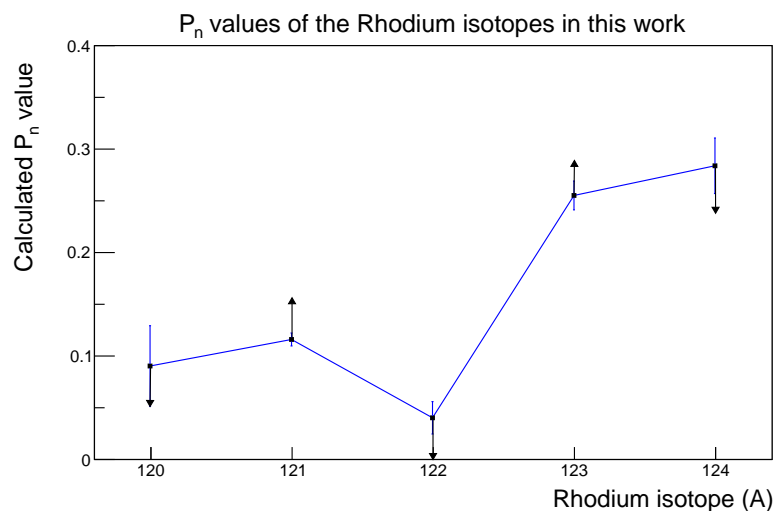


Figure 5: The upper and lower limits for even and odd mass rhodium isotopes determined in this work



## 5. Acknowledgements

This work was partially supported by the STFC UK (grant numbers ST/L005743/1 and ST/P005314) and UK Department of Business, Energy and Industrial Strategy (BEIS) via the National Measurement System. RS thanks the Nuclear Decommissioning Authority (NDA) for the award of an NDA Bursary. FGK acknowledges funding by the U.S. Department of Energy, Office of Nuclear Physics, under Contract No. DE-AC02-06CH11357.

## References

- [1] Yano Y 2005 *Proc. 2005 Part. Accel. Conf.* pp 320–324
- [2] Nishimura S, Lorusso G, Xu Z, Wu J, Gernhauser R, Jung H S, Kwon Y K, Li Z, Steiger K and Sakurai H 2013 *RIKEN Accel. Prog. Rep.* **46** 2013
- [3] Söderström P A *et al.* 2013 *Nucl. Instrum. Methods Phys. Res. Sect. B* **317** 649–652
- [4] Walters W B *et al.* 2004 *Phys. Rev. C* **70**(3) 034314
- [5] Lorusso G *et al.* 2015 *Phys. Rev. Lett.* **114**(19) 192501
- [6] Stoyer M A *et al.* 2007 *Nucl. Phys. A* **787** 455–462
- [7] Montes F *et al.* 2006 *Phys. Rev. C* **73** 1–9
- [8] Kameda D *et al.* 2012 *Phys. Rev. C* **86** 054319
- [9] Wang H *et al.* 2013 *Phys. Rev. C* **88**(5) 054318
- [10] Takeuchi S, Motobayashi T, Togano Y, Matsushita M, Aoi N, Demichi K, Hasegawa H and Murakami H 2014 *Nucl. Instrum. Methods Phys. Res. Sect. A* **763** 596–603